Published in final edited form as:
Nucl Instrum Methods Phys Res A. 2005 August 11; 548(1-2): 30–37.

X-ray microbeams: Tumor therapy and central nervous system research

F.A. Dilmanian[a,*], **Y. Qu**[b], **S. Liu**[b], **C.D. Cool**[c], **J. Gilbert**[a], **J.F. Hainfeld**[d], **C.A. Kruse**[c], **J. Laterra**[e], **D. Lenihan**[b], **M.M. Nawrocky**[a], **G. Pappas**[a], **C.-I. Sze**[c], **T. Yuasa**[f], **N. Zhong**[a], **Z. Zhong**[g], and **J.W. McDonald**[b,h,1]

a *Medical Department, Brookhaven National Laboratory, Upton, NY 11973, USA*

b *Department of Neurology and the Spinal Cord Injury Restorative Treatment and Research Program, Washington University, St. Louis, MO, USA*

c *Department of Pathology, University of Colorado Health Sciences Center, Denver, CO, USA*

d *Biology Department, Brookhaven National Laboratory, Upton, NY 11973, USA*

e *The Kennedy Krieger Institute, John Hopkins School of Medicine, Baltimore, MD 21205, USA*

f *Department of Bio-system Engineering, Yamagata University, Yamagata, Japan*

g *National Synchrotron Light Source, Brookhaven National Laboratory, Upton, NY 11973, USA*

h *Departments of Neurology, Neurological Surgery, Anatomy, and Neurobiology, and the Spinal Cord Injury Restorative Treatment and Research Program, W.U*

Abstract

Irradiation with parallel arrays of thin, planar slices of X-ray beams (microplanar beams, or microbeams) spares normal tissue, including the central nervous system (CNS), and preferentially damages tumors. The effects are mediated, at least in part, by the tissue's microvasculature that seems to effectively repair itself in normal tissue but fails to do so in tumors. Consequently, the therapeutic index of single-fraction unidirectional microbeam irradiations has been shown to be larger than that of single-fraction unidirectional unsegmented beams in treating the intracranial rat 9L gliosarcoma tumor model (9LGS) and the subcutaneous murine mammary carcinoma EMT-6. This paper presents results demonstrating that individual microbeams, or arrays of parallel ones, can also be used for targeted, selective cell ablation in the CNS, and also to induce demyelination. The results highlight the value of the method as a powerful tool for studying the CNS through selective cell ablation, besides its potential as a treatment modality in clinical oncology.

Keywords

Dosimetry; Synchrotron radiation; Micro-beam therapy

1. Introduction and background

1.1. X-ray microplanar beams

The technique of X-ray microbeam irradiation, i.e., exposing tissue to single-dose-fraction arrays of parallel, thin (25–90 μm) planes of synchrotron-generated X-rays (microplanar beams, or microbeams), was developed at the X17B1 superconducting wiggler beamline of

*Corresponding author. Tel.: +1 6313447696; fax: +1 6313445311. *E-mail address:* dilmanian@bnl.gov (F.A. Dilmanian)..
[1]Present address: The Kennedy Krieger Institute, John Hopkins School of Medicine, Baltimore, MD 21205.

the National Synchrotron Light Source (NSLS), Brookhaven National Laboratory (BNL) around 1990 [1,2]; it has also been studied at the European Synchrotron Radiation Facility (ESRF), Grenoble, France [3] since the mid-1990s. The properties of microbeams that make them a good candidate for tumor therapy are (a) their sparing effect on normal tissues, including the central nervous system (CNS) [2–17], and (b) their preferential damage to tumors, even when administered from a single direction [4,7,12,14]. These concepts are depicted in Fig. 1. The method is known as microbeam radiation therapy (MRT) [1].

1.2. The two microbeam effects and the method's therapeutic index: published results

The normal-tissue sparing effect of single-fraction microbeam arrays was established in the brain of the adult rat [2,4–7,12], the cerebellum of suckling rats [8], the CNS of duck embryos [10], the cerebellum of piglets [11], and the skin of the mouse [14] and the rat [15]. The preferential tumoricidal effect of microbeams was demonstrated in two tumor models. The first model was the intracranial rat 9LGS tumor that was treated using (a) a single parallel array of microbeams (called unidirectional irradiation, or irradiation with a co-planar array) [5,7,12], (b) two orthogonal arrays crossing at the tumor (bidirectional irradiation) [5–7], and (c) three orthogonal arrays crossing at the tumor (tridirectional irradiation) [6]. The second model was the subcutaneous murine mammary carcinoma EMT-6 tumor that was treated using two unidirectional irradiation methods [14]:

- co-planar microbeam arrays, and
- cross-planar arrays, in which two arrays are incident from the same direction on the target, one with horizontal microplanar beams and one with vertical ones.

Slatkin [18] recently discussed different methods of possible clinical microbeam irradiation. The animal studies suggested that single-fraction, unidirectional microbeams have a larger therapeutic index for treating the above tumors than do single-fraction unidirectional broad beams [12,14]. The therapeutic index is defined as the maximum dose tolerated by normal tissues divided by the minimum dose for ablating the tumor, or, alternatively, as ED50/TCD50, where ED50 and TCD50 are the doses that produce a 50% radiobiological effect in normal tissues (in our case, a damage) and a 50% effect in controlling tumors (in our case, ablating them), respectively.

The biological processes underlying the above two effects of microbeams are not well understood. For the sparing effect of microscopic beams in normal tissue, which Curtis et al. first established with deuteron beams [19,20] rather than with X-ray beams, we can confidently say that the effect involves the rapid regeneration of the tissue's microvessels from cells surviving outside the microbeams' direct paths (for microbeam arrays, this means survival in the ''valley dose'' regions, i.e., the spaces between individual microbeams). This effect was demonstrated in work at the ESRF wherein the vascular network of the chorio-allantoic membrane of the chicken embryo was observed in vivo following microbeam irradiation [13]. Furthermore, it also became clear that the CNS and the glial system somehow recover from the insult [2,7,8,11]. Our new studies, discussed in this paper [17,21–23], reveal more details of this recovery.

The preferential tumoricidal effect of microbeams is thought to be partly due to the failure of the tumor's microvessels to repair the damage inflicted by these beams, which could then lead to the loss of blood perfusion and tissue necrosis [7,12,14]. The effects might reflect major differences between the microvasculature of normal tissues and tumors in response to radiation [24,25], including (a) the rapid proliferation of endothelial cells in tumors which may render their microvessels more vulnerable to microbeam damage, and (b) the abnormal basement membrane in the tumor's vasculature [25].

2. CNS effects of microbeams

2.1. Earlier results on selective neuronal cell ablation by microplanar beams

Laissue et al. [4] and Slatkin et al. [2] were first to report targeted, selective ablation of granular cells in the rat's cerebellum with high-dose X-ray microplanar beams. Fischer 344 rats were irradiated anteroposteriorly (AP) with a microbeam array with 37 μm beam width and 75 μm on-center beam spacing. The array was arranged in alternating triplet microbeams delivering 1000 and 2500 Gy in-beam incident doses to the brain. The X17B1 beam was filtered with 0.25 mm Gd, producing a 48.5 keV half-power energy and a 16.3 mm tissue half-value layer. Therefore, on reaching the cerebellum, the in-beam in-depth doses were less than half the initial incident dose. Thirty days after exposure, the cerebella tissue was removed, stained with hematoxylin and eosin (H&E; staining the cell nucleus and cytoplasm, respectively), and studied [2]. Later microbeam studies at the NSLS and ESRF also reported such ablation of neuronal cells; the animal models were the cerebellum of the adult rat [7], suckling rat [8], and piglet [11].

2.2. Present studies of cell ablations in the CNS

Here we report mainly results from two studies in which the rat's brain was irradiated AP with high-dose microbeams. The first study (Experiment 1) used very narrow microbeams (27 μm), spaced 200 μm on-center at an 800 Gy in-beam incident dose; over a limited time we followed the course of microbeam-induced granular cell ablation in sections from the cerebellum, stained with hematoxylin [17]. In the second experiment we employed a single, much wider microplanar beam (270 μm) at 750 Gy dose, and followed the ablation of oligodendrocytes and astrocytes in the rat brain's white matter. We also briefly discuss a study of the rat's spinal cord irradiated with 270 μm wide high-dose microbeams to assess demyelination and remyelination, in addition to the loss and recovery of the glial cell populations. Experiment 1 was carried out in collaboration with Drs. Cool, Kruse, and Sze of University of Colorado Health Sciences Center (UCHSC). Experiment 2 was carried out in collaboration with both UCHSC and Dr. John McDonald and his group at Washington University, and the spinal cord study [21–23] was carried out in collaboration with Dr. John McDonald and his group.

3. Experimental design

3.1. Beam energy considerations

For a given synchrotron source the beam's energy is determined by the amount of beam filtration used. Because of the trade-off between the beam's energy and dose rate, the main consideration in choosing the filtration naturally is the dose rate needed for a particular study. However, even if the synchrotron source and the dose-rate requirement allow it, the beam's energy cannot be raised beyond the limit at which it increases the array's valley dose to an undesirable level in the normal tissue. This consideration is more important for smaller values of beam width and spacing (e.g., 30 and 100 μm, respectively).

To clarify this point, we present the findings from Monte Carlo simulations of dose distribution in a water phantom produced by a microbeam array of 30-μm beam width and 200 μm beam spacing (Fig. 2). The code used was the upgraded EGS4 [26–28], and the routine was similar to those used in the earlier studies at BNL [1,29]. The simulations show a single period of the array's dose distribution, from one beam's center to another. The phantom was 16 × 16 cm, and the array size was 30 × 30 mm, impinging on the phantom's flat side and being centered symmetrically about the cylinder's axis. The observation region was at the center laterally, and 7.5–8.5 cm deep into the phantom. The simulations were carried out with monochromatic beams of 75, 150, and 200 keV. An important feature of the resulting plots is the rounding of the edges of the beams at the top and the bottom of the fall-off curves; these effects are produced

by the finite range of the photoelectrons and Compton electrons, set in motion by the incident X-ray photons. These results clearly show that already at 150 keV, and unequivocally at 200 keV, these electrons produce considerable rounding of the edges of the valley dose region, although the value at the bottom of the valley in this configuration still is produced by the photoelectrons and Compton electrons of the scattered photons and not the incident ones. If these results are gradually extrapolated to higher beam energies, especially after reducing the beams' spacing (e.g., to 100 μm), an energy is soon reached at which the rounding of the valleys' edges dominates the entire valley dose. Because the valley dose in the normal tissue should be kept below the threshold dose for tissue damage, the effect sets an upper limit for the beam's energy for a given beam width/spacing. In general, 250 keV should be considered as an upper limit for microbeam configurations similar to those appearing in the literature.

3.2. Irradiation set-up

The studies presented here were carried out at the NSLS's X17B1 superconducting wiggler beam-line. The storage ring operated at 2.8 GeV and the superconducting wiggler operated at 4.3 T. The beam was filtered with 3.17 mm of silicon and 6.35 mm of copper, producing a half-power energy of about 120 keV and a dose rate of about 50 Gy/s at the site for the subject, about 30 m from the source.

3.3. Design of experiment 1

Male Fischer 344 rats, 200–225 g, were irradiated AP with a 10 × 10 mm unidirectional array of microbeams of 27 μm width, 200 μm spacing [17]. The beam was produced from a broad beam using a tungsten multislit collimator manufactured by Tecomet [30], the manufacturer of the multislit collimator used in our earlier works [14,15]. The collimator was 5 mm thick in the direction of the beam, and produced an array of vertical micro-planar beams, 1.5 mm high and up to 50 mm wide. The in-beam incident dose used was 800 Gy, attenuating to about 560 Gy at the depth of the cerebellum. Two rats were studied at the following times after exposure: 3 h, 2, 4, and 16 d. No acute dose effects were observed. The rats were euthanized, using a CO_2–O_2 mixture. Their brains were removed, fixed in formalin, and axial cuts of tissue were embedded in paraffin. Serial sections (5 μm) were made and stained with hematoxylin.

3.4. Design of experiment 2

The second experiment was designed to show the targeted ablation of oligodendrocytes and astrocytes in the white matter of the rat's brain. The animals were irradiated AP with a single, vertical microplanar beam 270 μm wide (actually, three 90 μm beams side-by-side) and 11 mm high at an entrance dose of 750 Gy. Following euthanasia of groups of animals at one week, three weeks, and three months by tissue perfusion with phosphate buffered saline (PBS) and then 10% buffered formalin, the brains were sectioned sagittally, embedded in paraffin, and sectioned at 5 μm. The sections were stained with immunofluorescent labeling specific to oligodendrocytes and astrocytes.

4. Results

4.1. Results of experiment 1

The results are shown in Figs. 3–7. The 3-h time-point cerebellum tissues stained with hematoxylin already showed the microbeams' paths as bands of cell with hyperchromatic nuclei (Fig. 3), representing neurons gradually undergoing necrotic death [17]. The staining for hyperchromatic cells was more intense at 2 d (Fig. 4), but by 4 d the density of these cells started to decrease (Fig. 5). By day 16, the beams' paths were represented by hypo-chromatic bands of missing nuclei in the tissue (Fig. 6). Fig. 7 shows a tissue section similar to that of Fig. 6 in which two intact capillary blood vessels are seen crossing these former microbeam

paths; this observation is evidence for the regeneration of the capillaries after irradiation. The banding effect in the cerebrum was visible, although much less pronounced (Fig. 8). This lesser response, which we had also previously observed in the microbeam-irradiated rat's brain, is partly attributed to the comparative paucity of neurons in the cerebrum; cerebral banding became visible only after 3 weeks.

4.2. Results of experiment 2

Fig. 9 shows the results of immunohistochemical studies of white matter tissue in the rat brain (midsagittal sulcus), one week after irradiation. The panel shows from left to right, immunofluorescent labeling for adenomatous polyposis coli (APC; oligodendrocytes; red), glial fibrillary acid protein (GFAP; astrocytes; green), Hoechst nuclear counterstaining (blues), and the triple overlay. The loss of putative oligodendrocytes (APC^+) and astrocytes ($GFAP^+$) within the beam's path and their preservation just outside it are clear. At two months (not shown) these cell populations were largely restored.

4.3. Microbeam-induced demyelination and subsequent remyelination in the rat's spinal cord

Male Fischer 344 rats were irradiated with a single microplanar beam, or up to 4 parallel ones, of a 270 μm wide beam at high doses including a 1000 Gy incident dose (about 750 Gy in-depth dose) [21–23]. Two weeks later, oligodendrocytes and astrocytes had been selectively ablated and myelin was destroyed in the microbeam's path, as detected by immunofluorescence techniques; at three months, uniform repopulations of the glial cells, and remyelination, were observed. No vascular damage was seen, and no axonal loss was detected of white matter [21–23]; therefore the tissue's cytological features were intact except for the early-stage loss of glial cells or myelin within the microbeam slice.

5. Discussion and conclusions

The body of evidence already appearing in the literature on microbeam effects studied in different normal and cancerous tissues points to the potential of microbeam in clinical radiation therapy. This potential is based on the remarkable tolerance of normal tissues to microbeams, and on the larger therapeutic index for MRT over conventional beams found in treating two types of malignant tumors. However, any particular application must overcome problems such as (a) keeping the valley dose adequately low in the normal tissue, which may not be easy for large and/or deeply seated tumors, (b) minimizing the effects of cardiosynchronous body pulsation, which might be achieved by administering the entire dose in a fraction of heart beat or by cardiac-gated irradiation and (c) mitigating the effects of a high dose to the proximal tissue that is needed because of the beams' relatively low energy, and thus more limited dose penetration to the tissue. The solutions may be in finding the right clinical applications, and the right irradiation geometries. MRT is currently considered one of the most exciting applications of synchrotron X-rays in medical research [3,31].

The potential of microbeams for CNS research is also very large, based on the findings presented here and by other investigators. In particular, our results show that microbeams can selectively ablate slices of neurons, oligodendrocytes, and astrocytes in the CNS because of the differential dose sensitivity of different cell types, without causing tissue necrosis. In other words, by adjusting the dose one can selectively ablate different cell types. Also, our results show that microbeams can induce temporary demyelination in two weeks without axonal or vascular damage, with remyelination following in 3 months post-irradiations. The effects are a further indication of the recovery of the normal tissue's microvasculature after exposure to microbeam irradiation, especially from transient damage to the capillaries. This recovery constitutes the basis for restoring the tissue's viability, and therefore its complete restitution; it signifies that the normal tissue remains viable (i.e., in terms of blood perfusion and metabolic

activities) even though slice(s) of neurons or glial cells were ablated (i.e., there is no ‘‘pan necrosis’’). Because no other method can ablate the glial cells and cause demyelination without concomitantly inducing some damage in the tissue’s structure, we conclude that microbeams offer a unique tool for studying the effects of selective removal of mitotic and non-mitotic cells in the CNS and other tissues.

Acknowledgements

We thank T. Bacarian, M.E. Berens, A. Feldman, C. Garibotto, T. George, J. Giordano, S. Hussain, Z. Hussain, Y. Kublanskaya, S. Leroy, R. Maehara, P. Mortazavi, A. Nithi, I. Orion, S. Rafiq, B. Ren, E.S. Rosenzweig, J.K. Robinson, A. Ruvinskaya, T. Steidinger, S. Thomas, J. Welwart, D. Williams, A.D. Woodhead, and R. Yakupov for their valuable assistance. These studies were funded by the Nextsteps Foundation, IL (JWM), the National Institute of Health NINDS grants NS37927, NS40520, NS39577 (JWM) and NS43231 (FAD), and the Office of Biological and Environmental Research, U.S. Department of Energy. This research was carried out at the NSLS which is supported by the U.S. Department of Energy, Division of Materials Sciences and Division of Chemical Sciences, under Contract No. DE-AC02-98CH10886.

References

1. Slatkin DN, Spanne P, Dilmanian FA, Sandborg M. Med Phys 1992;19:1395. [PubMed: 1461201]
2. Slatkin DN, Spanne P, Dilmanian FA, Gebbers JO, Laissue JA. Proc Nat Acad Sci 1995;92:8783. [PubMed: 7568017]
3. Thomlinson W, et al. Cell Mol Biol 2000;46(6):1053. [PubMed: 10976863]
4. Laissue J, Spanne PO, Dilmanian FA, Gebbers JO, Slatkin DN. Schweiz med Wschr 1992;122:1627.
5. Slatkin DN, Dilmanian FA, Nawrocky NM, Spanne P, Gebbers JO, Archer DW, Laissue JA. Rev Sci Instrum 1995;66:1459.
6. Slatkin, DN.; Cole, SM.; Dilmanian, FA.; Joel, DD.; Micca, PL.; Nawrocky, MM.; Wu, X-Y.; Spanne, P.; Gebbers, J-O.; Laissue, JA. Two- and three-dimensional microbeam radiation therapy [MRT] of malignant brain tumors in rats, 1994 Annual Activity Report of The National Synchrotron Light Source. Rothman, EZ., editor. BNL 52445, May 1995, p. B-110.
7. Laissue JA, Geiser G, Spanne PO, Dilmanian FA, Gebbers JO, Geiser M, Wu XY, Makar MS, Micca PL, Nawrocky MM, Joel DD, Slatkin DN. Int J Cancer 1998;78:654. [PubMed: 9808538]
8. Laissue, JA.; Lyubimova, N.; Wagner, HP.; Archer, DW.; Slatkin, DN.; Di Michiel, M.; Nemoz, C.; Renier, M.; Brauer, E.; Spanne, PO.; Gebbers, J-O.; Dixon, K.; Blattmann, KH. Microbeam radiation therapy; Medical Applications of Penetrating Radiation. SPIE Conference Proceeding, vol. 3770, Medical Applications of Penetrating Radiation. pp. 38–45. Microbeam radiation therapy. In: Medical Applications of Penetrating Radiation (H.B. Barber and H. Roehrig, Eds.), SPIE Conference Proceeding, vol. 3770; Bellingham, WA, SPIE.. 1999. p. 38-45.
9. Schweizer PM, Spanne P, Di Michiel M, Jauch U, Blattmann H, Laissue JA. Int J Radiat Biol 2000;76:567. [PubMed: 10815638]
10. Dilmanian FA, Morris GM, Le Duc G, Huang X, Ren B, Bacarian T, Allen JC, Kalef-Ezra J, Orion I, Rosen EM, Sandhu T, Sathé P, Wu XY, Zhong Z, Shivaprasad HL. Cellular Molec Biol 2001;47:485. [PubMed: 11441956]
11. Laissue, JA., et al. The weanling piglet cerebellum: a surrogate for tolerance to MRT (microbeam radiation therapy) in pediatric neuro-oncology. In: Barber, HB.; Roehrig, H.; Doty, FP.; Schirato, RC.; Morton, EJ., editors. Penetrating Radiation Systems and Applications III, SPIE Conference Proceeding, vol. 4508; Bellingham, WA, SPIE. 2001. p. 65-73.
12. Dilmanian FA, et al. Neuro-Oncology 2002;4:26. [PubMed: 11772430]
13. Blattmann, H.; Burkard, W.; Di Michiel, M.; Brauer, E.; Stepanek, J.; Bravin, A.; Gebbers, J-O.; Laissue, JA. Microbeam irradiation of the chorio-allantoic membrane (CAM) of the chicken embryo, Paul Scherrer Intstitute (PSI) Scientific Report 2001/vol. II (Life Sciences). ISSN 1423-7318, March 2002, p. 73.
14. Dilmanian FA, Morris GM, Zhong N, Bacarian T, Hainfeld JF, Kalef-Ezra J, Brewington LJ, Tammam J, Rosen EM. Radiat Res 2003;159:632. [PubMed: 12710874]
15. Zhong N, Morris GM, Bacarian T, Rosen EM, Dilmanian FA. Radiat Res 2003;160:133. [PubMed: 12859223]

16. Dilmanian FA, Kalef-Ezra J, Petersen MJ, Bozios G, Vosswinkel J, Giron F, Ren B, Yakupov R, Antonacopoulos G. Cardiovasc Radiat Medicine 2003;4:139.

17. Dilmanian, FA.; Hainfeld, JF.; Kruse, CA.; Cool, CD.; Sze, C-I.; Berens, ME.; Maehara, R.; Feldman, A.; Zhong, N. Direct granular cell death in the rat cerebellum observed in the paths of very high dose X-ray microbeams. In: Corwin, MA.; Ehrlich, SN., editors. National Synchrotron Light Source Activity Report 2002; May 2003; Abstract Dilm0593.

18. Slatkin DN. Phys Med Biol 2004;49:N203. [PubMed: 15285266]

19. Curtis HL. Radiat Res Suppl 1967;7:250. [PubMed: 6058661]

20. Curtis HL. Radiat Res Suppl 1967;7:258. [PubMed: 6058662]

21. Dilmanian, FA.; Qu, Y.; Liu, S.; Hainfeld, JF.; Steidinger, T.; Gilbert, J.; Yakupov, JR.; Sze, C-I.; McDonald, JW. Selective demyelination with minimal axonal and vascular damage induced by high-dose synchrotron-generated X-ray microbeams; Presented at the 2004 Annual Meeting of the Radiation Research Society; 24–27 April, 2004; St. Louis, MO. 102 (unpublished).

22. Qu, Y.; Dilmanian, YFA.; Lenihan, D.; Liu, DS.; Steidinger, T.; Gilbert, J.; Yakupov, R.; Sze, C-I.; McDonald, JW. A novel method for targeted, selective, axon sparing, demyelination and targeted cell ablation; Presented at the 34th Annual Meeting of Society for Neuroscience; 23–27 October, 2004; San Diego, California. (unpublished).

23. Dilmanian FA, Qu Y, Rosenzweig ES, Lenihan D, Liu S, Steidinger T, Vadivelu S, Gilbert J, Yakupov R, Sze CI, McDonald JW. Selective demyelination with minimal axonal damage induced by high-dose synchrotron-generated X-ray microbeams. Glia. (submitted).

24. Garcia-Barros M, Paris F, Cordon-Cardo C, Lyden D, Rafii S, Haimovitz-Friedman A, Fuks Z, Kolesnick R. Science 2003;300(5622):1155. [PubMed: 12750523]comment in: Science 2003, 302 (5652):1894, 2003; author reply 1894. 2003

25. Baluk P, Hashizume H, McDonald DM. Curr Opin Genet Dev 2005;15:102. [PubMed: 15661540]

26. Nelson, WR.; Hirayama, H.; Rogers, DWO. The EGS4 Code System, SLAC, 265. 1985.

27. Namito, Y.; Ban, S.; Hirayama, H. Nucl Instr and Meth in Phys Res 332. 1993. p. 277

28. Namito Y, Ban S, Hirayama H. Phys Rev 1995;51:3036.

29. Orion A, Rosenfeld B, Dilmanian FA, Telang F, Ren B, Namito Y. Phys Med Biol 2000;45:2497. [PubMed: 11008951]

30. Tecomet. Woburn; Massachusetts:

31. Lewis R. Phys Med Biol 1997;42:1213. [PubMed: 9253036]

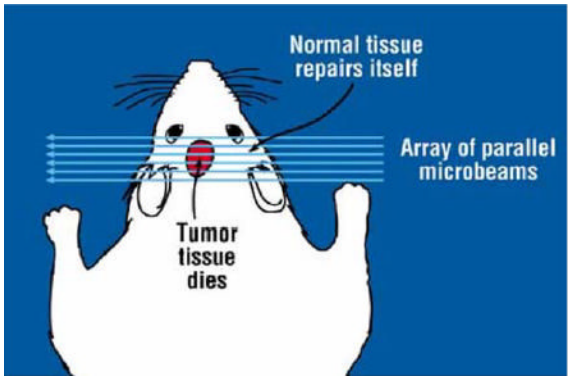

Fig. 1.
Schematic view of irradiating a tumor with an array of parallel microbeams. The figure indicates the sparing effect of microbeams in normal tissue, and their preferential tumoricidal effect.

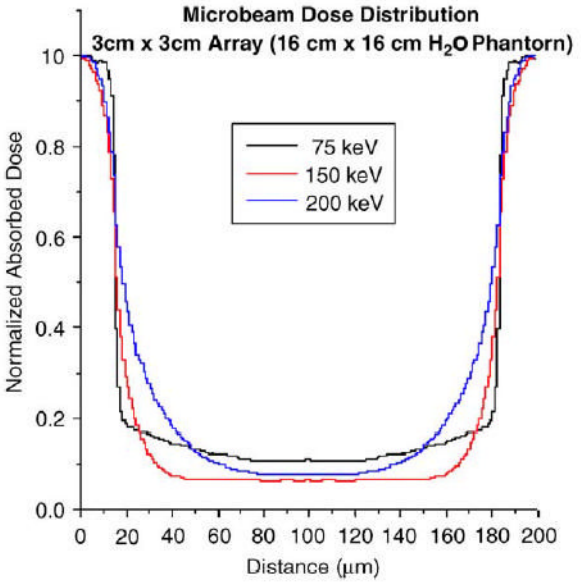

Fig. 2.

Monte Carlo simulations of the dose distribution from an array of parallel microbeams in a cylindrical water phantom using the EGS4 code of photon- and electron-transport. The figure represents the dose distribution for one complete period of the array.

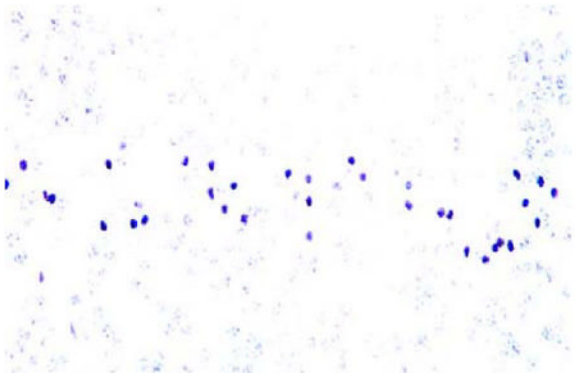

Fig. 3.
Path of a microbeam in the cerebellum 3 h post-irradiation seen as darkened cerebella granular cells (400 ×).

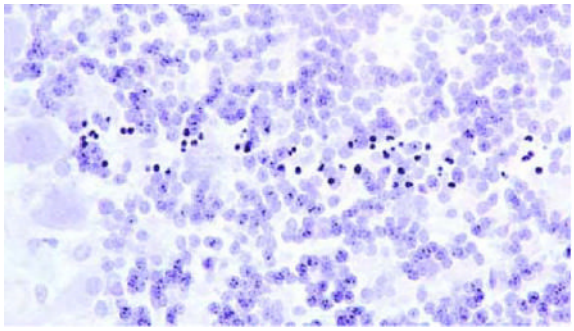

Fig. 4.
Microbeam's path seen in the cerebellum 2 d post-irradiation (400 ×).

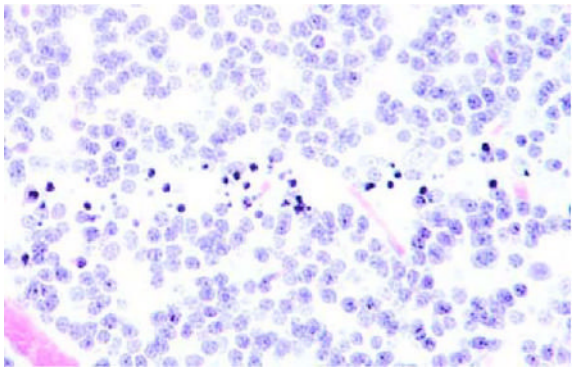

Fig. 5.
Microbeam's path in the cerebellum 4 d post-irradiation. Some neurons have disappeared (400 ×).

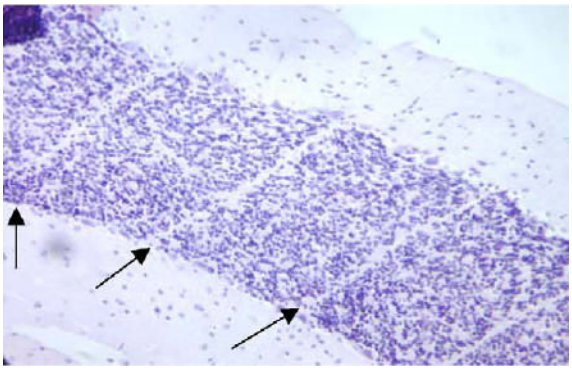

Fig. 6.
Microbeam pattern of banding seen in the cerebellum 16 d post-irradiation. Almost all neurons had disappeared, leaving a strong white band (arrows) (200 ×).

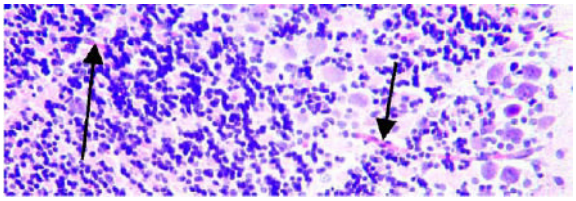

Fig. 7.
Similar to Fig. 6, but also showing two undamaged capillary blood vessels crossing the microbeam-induced tracks (arrows) (200 ×).

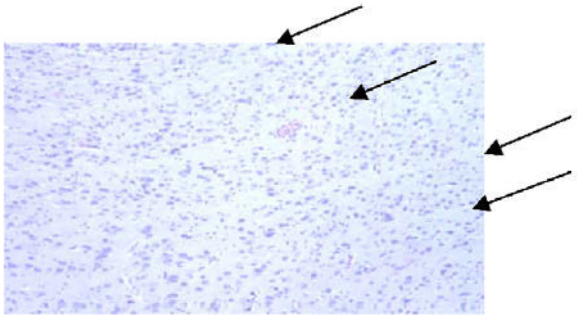

Fig. 8.
Microbeam pattern of banding seen in the cerebrum 3 weeks post-irradiation (arrows) (200 ×).

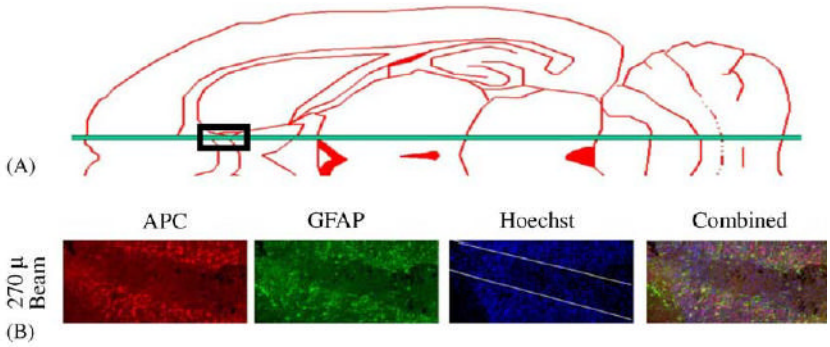

Fig. 9.

Schematic horizontal section of the rat brain showing the position of the microbeam just lateral to the midsaggital sulcus. Loss of putative oligodendrocytes (APC+) and astrocytes (glial fibrillary acidic protein, GFAP+) one week after exposure to a 270 μm wide, 650 Gy microbeam in the white matter of the rat brain (midsaggital sulcus) (work carried out in collaboration with John McDonald et al., Washington University).